The Extractive Industries and Society 20 (2024) 101526

Contents lists available at ScienceDirect

The Extractive Industries and Society

journal homepage: www.elsevier.com/locate/exis

Original article

An analysis of the impact of CO_2 emissions from deforestation and mining in Madre de Dios, Perú

Umut Mete Saka [a,*], Klaus Pacheco-Hague [b], Sebnem Duzgun [b], Nicole Smith [b]

[a] Computer Science, Colorado School of Mines, 1500 Illinois St. Golden, 80401, CO, USA
[b] Mining Engineering, Colorado School of Mines, 1500 Illinois St. Golden, 80401, CO, USA

ARTICLE INFO

Keywords:
CO2 emissions
Artisanal and small-scale gold mining
Deforestation
Madre de Dios
Carbon density
Carbon capture

ABSTRACT

The Madre de Dios Region of Peru faces significant deforestation largely due to a surge in artisanal-small scale gold mining (ASGM), propelled by rising gold prices. This study evaluates the full scope of ASGM activities on net CO_2 emissions, accounting for both the deforestation that converts forests into mining territories and the emissions directly resulting from mining and transportation activities. By applying kriging to a comprehensive dataset, we determined the carbon content of the region and the annual loss of CO_2 capture due to deforestation. Our analysis also incorporates emissions from the Interoceanic highway, which has contributed to the mining boom. The findings indicate a total net CO_2 emission of 429.9 Gigagrams (Gg) per year, underscoring the critical environmental challenge these activities pose. Our study highlights the need for immediate and effective reclamation efforts, including reforestation with indigenous carbon-rich trees, as a counterbalance to the environmental damage inflicted. These efforts are essential to mitigate the adverse impacts and support the global movement towards net-zero emissions.

1. Introduction

Greenhouse gas (GHG) emissions are a critical issue, contributing to global warming and climate change and the overall sustainability of the environment. Mining substantially contributes to GHG emissions, although the extent of this varies depending on the type and scale of mining and the specific minerals being extracted. GHG emissions from mining primarily result from extraction, mineral processing, and related activities such as transportation and energy consumption. The mining industry contributes an estimated 2 to 3 percent of global CO_2 emissions, emphasizing the importance of reducing emissions from this sector (Fritz et al., 2023).

Artisanal and small-scale gold mining (ASGM) is more labor- and energy-intensive than large-scale industrial mining (Fritz et al., 2023). It is a critical sector to examine when assessing GHG emissions from mining. While ASGM supports millions of livelihoods in numerous developing countries, it has significant environmental costs, including deforestation and mercury pollution (Espin and Perz, 2021; Salo et al., 2016). In particular, ASGM in the Amazon Region of Peru elevates these impacts, as deforestation reduces the carbon capture potential, and mercury emissions, fuel usage, and transportation increases GHG emissions. Understanding GHG emissions from ASGM is necessary to develop global net zero carbon emission strategies.

Two recent studies have quantified the mercury use per gram of gold produced from ASGM in the Amazon Region. Aranoglu et al. (2022) used field data and constructed system dynamics models to estimate that 1.15 g of mercury was released per gram of gold produced and 8.09 L of fuel was consumed per gram of gold produced in Madre de Dios (MdD). (Fritz et al., 2023) surveyed mercury and energy use by visiting mining sites in Brazil's Tapajós River basin of the Amazon Region. They estimated that the amount of mercury used per gram of gold extracted was 1.7 g. They concluded that ASGM activities contribute to climate change due to the energy consumption involved, releasing approximately 16,000 kg of CO_2 equivalent per kilogram of gold. Nevertheless, these studies overlook how and to what extent the loss of carbon capture potential from deforestation caused by mining contributes to GHG emissions in Amazon Regions. A more comprehensive methodology is required to establish a more holistic approach to mitigation.

Madre de Dios, a region of Perú in the Amazon Forest, is under severe deforestation threat, initially due to agriculture and, more recently, gold

* Corresponding author.
E-mail addresses: saka@mines.edu (U.M. Saka), kpachecohague@mines.edu (K. Pacheco-Hague), duzgun@mines.edu (S. Duzgun), nmsmith@mines.edu (N. Smith).

https://doi.org/10.1016/j.exis.2024.101526
Received 28 April 2024; Received in revised form 7 August 2024; Accepted 30 August 2024
Available online 8 September 2024

mining (Nicolau et al., 2019). Notably, the increase in gold prices after the 2008 global economic crisis boosted gold production in MdD (Asner and Tupayachi, 2016), where most ASGM in Perú occurs (Swenson et al., 2011). Furthermore, the Interoceanic Highway was completed in 2011 and connects Perú to Brazil, providing greater access to MdD and opening new areas for gold exploitation (Nicolau et al., 2019). Additionally, the highway is a notable source of emissions with fossil fuel powered vehicles passing over it. The majority of gold mining operations in MdD are carried out in the Southeastern part of the region, close to Puerto Maldonado, the largest city in the region, geographically located around the confluence of the Madre de Dios, Inambari, and Colorado River (Asner and Tupayachi, 2016; Caballero Espejo et al., 2018; Csillik and Asner, 2020; Swenson et al., 2011). The location of MdD in Peru deforested (mining) areas and highways can be depicted from Fig. 1.

This study assesses the environmental impact of artisanal and small-scale gold mining (ASGM) operations in the Madre de Dios (MdD) region. Our focus was to quantify the CO_2 emissions from mining activities, the traffic on the Interoceanic highway, and the loss of CO_2 capture capacity due to deforestation. Utilizing a geostatistical method applied to a comprehensive dataset of tree observations, we estimated the carbon content and the consequent emissions attributable to anthropogenic activities in MdD. We included emissions from the primary industrial activity—gold mining—covering both ASGM and large-scale operations by calculating the power emission factors for the typical machinery employed. Additionally, we considered vehicular emissions on the Interoceanic highway based on fuel consumption data. Our findings reveal significant environmental costs associated with these activities. We argue that these costs are not adequately accounted for in the current regulatory framework, and therefore, we propose policy recommendations based on our emissions model. We conclude by emphasizing the urgent need for revised environmental strategies to mitigate the adverse effects of gold mining and protect the ecological integrity of MdD.

The correlation between gold prices and mining activities and its connection to mercury import and use and deforestation was investigated by (Swenson et al., 2011); an estimation for the role of land cover change and soil erosion on river transport of Hg is provided by (Diringer et al., 2020), the density of Carbon content in the area and loss due to deforestation is calculated by (Csillik and Asner, 2020) and (Asner et al., 2010), using satellite imagery; the forest loss and its position within and outside Indigenous territories, protected areas, mining concessions, and reforestation concessions is mapped by (Nicolau et al., 2019) using spectral mixture analysis; annual changes in the forest cover is assessed by (Asner and Tupayachi, 2016) using high-resolution satellite imagery. An average carbon density of 91.9 Mg and 83.9 Mg per hectare in Madre de Dios is estimated in the results of (Asner and Tupayachi, 2016) and (Csillik and Asner, 2020), respectively.

Extensive research on deforestation in the region was conducted by (Caballero Espejo et al., 2018), who detected the deforested areas over 34 years, from 1984 to 2017, where yearly changes in the forest area are depicted using remote sensing. Continuously, they extend their findings by detecting the land use of the deforested areas, specifying highly and minimally mechanized mines, as shown in Fig. 2. They calculate deforestation of 95,751 hectares due to gold mining activities within these years. A staggering 64,586 hectares of this happened in the last seven years (2010–2017).

The paper's organization is as follows: Section 2 explains the materials and methods in detail, while Sections 3 and 4 provide the results and discussion, respectively.

2. Methods

Considering the spatial dimension of the mining operations over geographical regions, it is vital to determine the exact study area. We used data availability and concentration of human activities and deforested areas as our criteria to do this. The outline of the methodology is provided in Fig. 3. Stage 1 included selecting the study region; in Stage 2, we collected the relevant data. In Stage 3, we quantified the CO_2 capture loss by estimating the carbon content in the region and estimating the loss of carbon capture due to deforestation. We also estimated the carbon emissions from mining and transportation. Finally, in Stage 4, we calculated the net carbon emissions by combining our calculations from Stage 3.

2.1. Selection of study region (stage 1)

In selecting our study area, we decided on the Madre de Dios (MdD) region of Peru, renowned for its biodiversity and its high deforestation rate linked to mining and agricultural activities. Madre de Dios spans an area of approximately 85,000 sq. kilometers and is home to a population of over 140,000. An estimated 50,000 miners are directly involved in the industry that drives the economy of MdD, gold mining (Leiva, 2022), which has a significant footprint on the local environment. A major infrastructural feature is the Interoceanic Highway, stretching for more than 400 km within the region, facilitating transport but also contributing to the area's environmental challenges. The selected study area is defined based on the available data on these human activities, focusing on the zones most affected by deforestation, as detailed in Section 2.2. This region was chosen for its critical need for environmental monitoring and the availability of comprehensive data sets that allow for an in-depth analysis of human-induced environmental changes. Our geographical boundaries were drawn to encompass the intense interaction between anthropogenic activities and the natural landscape, providing a representative snapshot of the pressures on the MdD ecosystem.

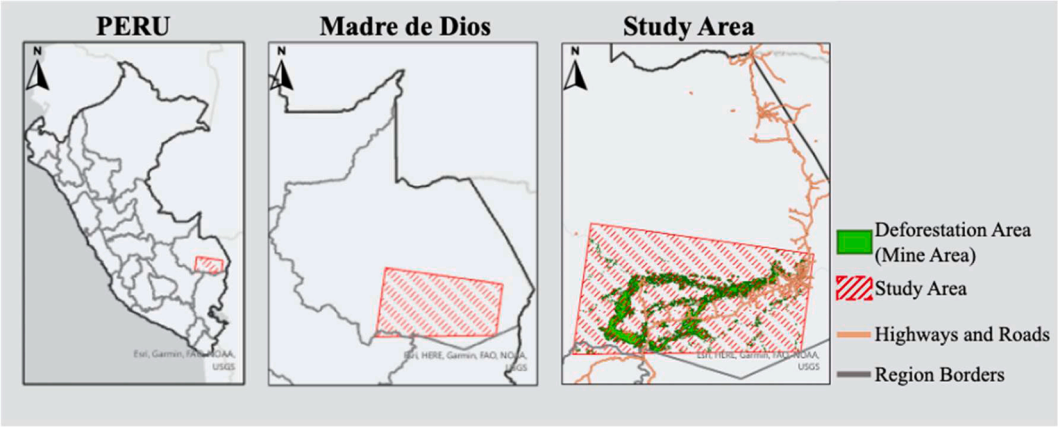

Fig. 1. Location of MdD in Perú in left, location of study area in Madre de Dios in middle, roads and deforestation (mining) areas in right.

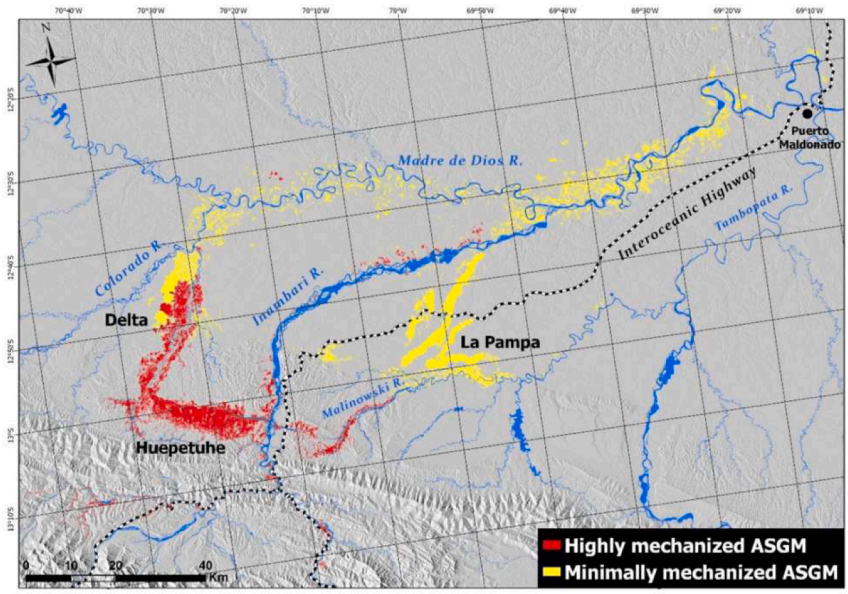

Fig. 2. Deforested areas, replaced by highly and minimally mechanized mines, adapted from Espejo et.al., 2018 *(Caballero Espejo et al., 2018)*.

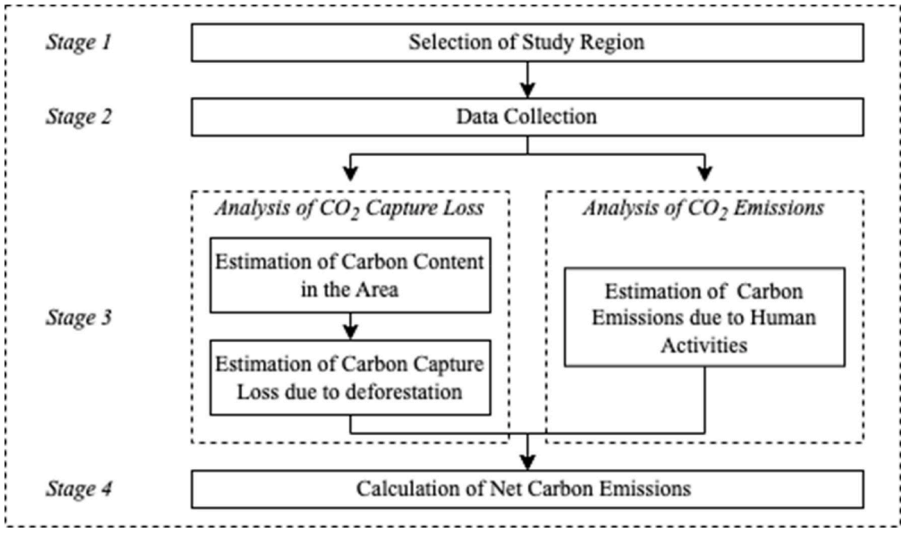

Fig. 3. Methodology flowchart.

2.2. Data collection (stage 2)

In our methodology, we utilized the findings of (Caballero Espejo et al., 2018) as a foundational reference to detect the size and geo-location of deforested lands and mining operations within the MdD. Their study, which identified deforestation zones and classified types of gold mining operations, served as the initial mapping from which we further developed our analysis. As illustrated in Fig. 2, the once-forested areas are now marked as sites of mining-induced deforestation. We incorporated these findings into our study by geo-referencing these areas in Fig. 4, labeled as 'Deforestation observation area', to quantify the spatial extent of both minimally and highly mechanized mining operations. Our calculations, while generally aligning with those of Caballero Espejo et al., exhibit a minor deviation of approximately 4 %. This deviation arises from the granularity differences in their visuals, yet it provides a reliable baseline for estimating the current magnitude of mining and deforestation within our study boundaries.

We utilized the Aarhus University Palm Transect Database (Balslev, 2016), which contains 32,521 individual tree observations within the region, detailing each tree's exact location and species (Fig. 4). Our study area is defined by the overlap of the Tree Observation Area and the Deforestation Observation Area, as depicted in Fig. 4 with red, which encompasses most mining operations within the Madre de Dios Region, covering 17,314 km^2. Fig. 1 illustrates the study area's position relative to the broader MdD region and Peru, highlighting the impact of mining operations on deforestation and the role of the Interoceanic Highway and its connecting roads.

To quantify the effect of transportation in Perú, we obtained highway statistics that contain vehicle toll count from the Supervisory Agency for Investment in Transport Infrastructure in Perú, OSITRAN (https://www.ositran.gob.pe/anterior/). To determine the emission values, we used power emission factors of 8.78 Kg/Gallon (2.32 Kg/Lt) for gasoline and 10.21 Kg/Gallon (2.69 Kg/Lt) for diesel (Environmental Protection Agency, 2023).

The variety of suppliers, brands, and types of equipment used, and the lack of government records make it difficult to determine the exact equipment employed in the field. Thus, we acquired a list of the standard equipment utilized in the area from a mining equipment specialist

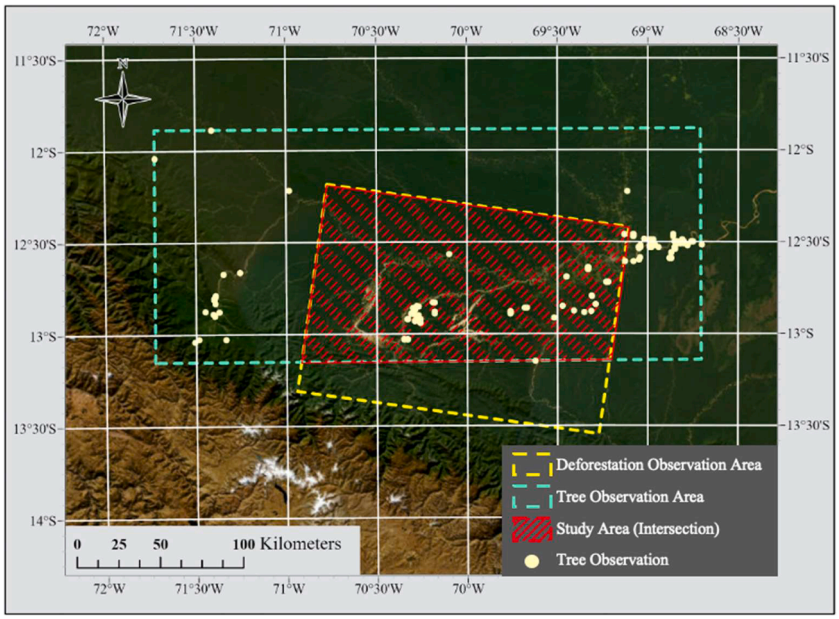

Fig. 4. Study area.

(Interview 1, 2023), a mining engineer with over 18 years of experience in equipment technology for surface and underground mines in Peru.

2.3. Estimation of emissions

The emissions in the study area were analyzed according to two variables: (i) The loss of CO_2 capture due to deforestation and (ii) emissions due to human activities. To assess the loss of CO_2 capture due to deforestation, we first had to quantify the potential CO_2 capture of a standing forest in this region. However, the CO_2 capture of trees is rarely studied in the literature, and the yearly CO_2 capture amount of the tree types in our study area is unavailable. Due to this limitation, we estimated the accumulated carbon content of the trees sourced by captured CO_2 and further predicted the loss of CO_2 capture, dividing this step into two, as described in Fig. 3.

The CO_2 emissions within the study area were quantified based on two primary variables: (i) the loss of CO_2 capture attributed to deforestation and (ii) emissions from human activities, specifically mining operations and transportation. It is essential to acknowledge that while other human activities may also contribute to CO_2 emissions, our focus is narrowed to these two significant sources due to their predominant impact in the region. To evaluate the CO_2 capture potential lost due to deforestation, we began by estimating the baseline CO_2 sequestration capability of the extant forest. However, the yearly CO_2 sequestration rates for the tree species in our area are sparsely documented in existing research. This gap required us to estimate the overall carbon content of the forest, derived from the CO_2 absorbed by trees, to approximate the decrease in CO_2 capture resulting from deforestation. This methodological approach, though indirect, provides a viable means to infer the loss of CO_2 capture and is detailed in two phases in Fig. 3.

2.3.1. Estimation of carbon content

Our analysis acknowledges the inherent variability in tree carbon content, which can be influenced by many factors such as height, age, and health conditions. We incorporated a range-based approach (min-average-max) to accommodate this variability and enhance the robustness of our carbon content estimates, we incorporated a range-based approach (min-average-max). We used tree specifications from (Henderson et al., 1995), which provide values as ranges rather than precise measurements, to input into the regression models developed by (Avalos et al., 2022). While not every species in our dataset matched the ones in their models, we could estimate the carbon content for 13 species at the genus level using their approach, utilizing 20,236 tree observations to estimate the carbon content.

By inputting the maximum, mean, and minimum values from Henderson's ranges, we generated estimates representing potential extremes (worst and best-case scenarios) and the mean likelihood (average scenario) of the carbon content for each species. This approach not only reflects the natural distribution of tree carbon content but also provides a comprehensive view that accounts for the best, average, and worst outcomes.

Although (Avalos et al., 2022) found that the model performances were quite similar, we observed that using a single point value rather than a range could lead to unrealistic estimates. To mitigate this, we applied all models compared by Avalos et al. to our data. This approach worked for 12 of the 13 species analyzed. For one species, Euterpe Precatoria, the models did not produce viable estimates for the best- and worst-case scenarios, generating implausible results. The implausibility in estimates is likely due to the lack of a larger sample set, especially with a wider range of sizes (Avalos et al., 2022). Thus, for this particular species, we used only the mean value for all three scenarios to ensure consistency in our estimates.

The chosen models, input parameter ranges (stem diameter or height) and resulting Carbon Content per tree for each species are visible in Table 1.

The remaining 20,236 observations allow us to estimate the average carbon content value over the tree observation area shown in Fig. 4. To estimate the loss of carbon content in the deforested areas, we treated the carbon content values of tree observations as spatially continuous data and applied the geostatistical method of Kriging interpolation to estimate the carbon content loss in the study area. By optimizing model parameters using leave-one-out cross-validation, we selected the universal Kriging with constant trend removal and a spherical semivariogram for all three models. We incorporated the Range and Sill values into our models, obtaining Root Mean Square Errors (RMSE) and Standardized RMSE (SRMSE) values through cross-validation. These values are presented in Table 2.

Kriging provided us with a prediction for the carbon content of a single tree in each cell, in our case 10 m by 10 m (100 m^2). To visualize these cells, we provide the Kriging maps of each case in Fig. 5, which shows the predicted tree carbon content in each cell for each case.

The variability and quantification of trees and tree species in the

Table 1
Models to estimate carbon content (Ln(C); kg), in four genus of neotropical palms, adapted from (*Avalos et al., 2022*).

Species	Model Ln(C)	Stem diameter Min-Ave-Max (cm)	Height Min-Ave-Max (m)	Carbon content Min-Ave-Max (Kg)
E. precatoria	-1.5 + 0.38*Diam	13.5 (Ave)	–	37.71
G. brevispatha	-1.2 + 0.41*H_{bc}	–	1 - 2.5 - 4	0.45 - 0.84 - 1.55
G. brongniartii	-1.2 + 0.41* H_{bc}	–	0.3 - 0.65 - 1	0.34 - 0.39 - 0.45
G. camana	-1.2 + 0.41* H_{bc}	–	0.3 - 1.15 - 2	0.34 - 0.48 - 0.68
G. deversa	-1.2 + 0.41* H_{bc}	–	1 - 2.5 - 4	0.45 - 0.84 - 1.55
G. interrupta	-1.2 + 0.41* H_{bc}	–	1 - 5.5 - 10	0.45 - 2.87 - 18.17
G. macrostachys	-1.2 + 0.41* H_{bc}	–	0.1 - 0.5 - 1	0.31 - 0.37 - 0.45
G. maxima	-1.2 + 0.41* H_{bc}	–	1 - 4 - 7	0.45 - 1.55 - 5.31
G. stricta	-1.2 + 0.41* H_{bc}	–	0.5 - 1.75 - 3	0.37 - 0.62 - 1.03
I. deltoidea	-4.43 + 2.48*Ln(Diam)	24 - 30 - 36	–	31.55 - 54.87 - 86.24
S. exorrhiza	-1.64 + 2.16*Ln(H_{bc})	–	8 - 14 - 20	17.32 - 58.00 - 125.31
S. salazarii	-1.64 + 2.16*Ln(H_{bc})	–	7 - 11.5 - 16	12.98 - 37.92 - 77.38

E.: Euterpe, G.: Geonoma, I.: Iriartea, S.: Socratea.
Diam: Stem Diameter (cm), H_{bc}: Height at the base of the crown (m).

Table 2
Model parameters and cross validation results of Kriging models.

Model data	Range	Sill	RMSE	SRMSE
Best case	0.0151	36.88	11.35	1.21
Average case	0.0151	163.1	16.34	1.24
Worst case	0.0151	280.13	27.52	1.27

Amazon were computed by using a large data set, yielding an estimated median tree distribution of 565 trees per hectare (10,000 m^2). This is equivalent to 5.65 trees per 100 m^2, our cell size. Therefore, using this as a guide, we multiplied each cell value by 5.65 and calculated the total carbon content in the area.

2.3.2. *Estimation of CO_2 capture loss*

To estimate a tree's annual carbon sequestration rate, it is essential to consider its age, as carbon accumulation occurs throughout a tree's life. For the common palm species, we have assumed the median age of the

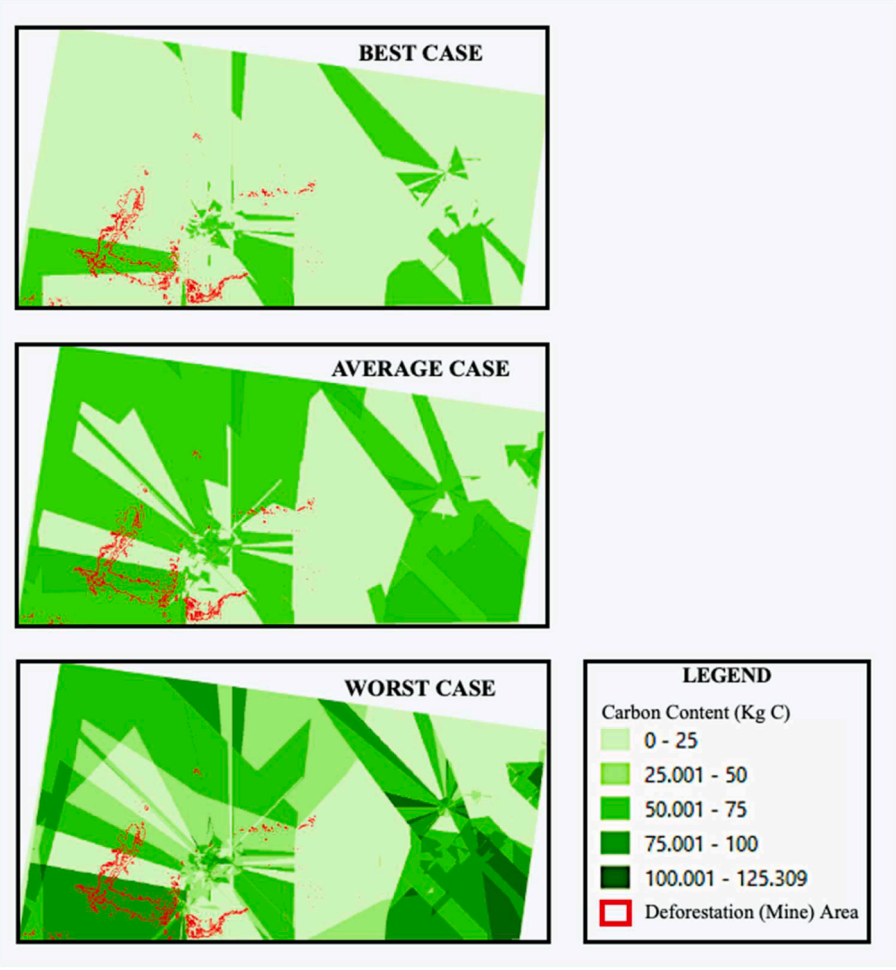

Fig. 5. Kriging maps of best case, average case, and worst case models.

trees in our study area to be approximately 50 years (Isaza et al., 2017). This age is a basis for calculating the yearly carbon capture by dividing the total carbon content, which is built over the tree's life, by this average age. Given that carbon (C) bonds with oxygen (O_2) to form carbon dioxide (CO_2) and considering the molecular weight of CO_2 is 44 g/mole compared to 12 g/mole for carbon alone, we can determine that the tree's carbon content represents the storage of 3.6667 times that weight in CO_2.

Consequently, we estimate the CO_2 Capture loss (CO_2), using carbon content (CC) by equation 1 given as:

$$CO_2 = CC * \frac{3.667}{50}$$

2.3.3. Estimation of carbon emissions due to mining and transportation

Human activities contributing to CO_2 emissions are manifold, including industrial, agricultural, transportation, and population components. As discussed before, mining constitutes the major industry in the region, and the Interoceanic Highway is the most important means of land transport in the region. We are aware of the emission aspects of population and agriculture; however, we limit our work to these two significant sources.

2.3.3.1. Mining operations. Two types of mining operations, minimally (artisanal-small) and highly mechanized (medium-large scale), are common in the area (Caballero Espejo et al., 2018). Minimally mechanized mining is mainly the alluvial gold mining process consisting of sediment extraction, sediment washing, gold gravel recovery, and amalgamation with mercury (Aranoglu et al., 2022).

Law No 27651, *"Law on Formalization and Promotion of Small Mining and Artisanal Mining"* (*"Ley de Formalización y Promoción de la Pequeña Minería y la Minería Artesanal - LEY N° 27651"*) of 2017 created the definitions for small-scale and artisanal-mining producers. These categories have varied over the years, but currently, small-scale miners are allowed to mine an area of up to 2000 hectares and process 350 Metric Tons of ore per day, while artisanal miners can mine an area of up to 1000 hectares and process 25 Metric Tons of ore per day. We treat artisanal and small mining as minimally and highly mechanized mines, respectively, considering all the mining operations in the region fall into these two categories. We assume an average size of between 500 and 1500 hectares, or 5 Km^2 and 15 Km^2, respectively.

In minimally mechanized mining operations, miners employ *tracas*—a sediment extraction apparatus—mounted on rafts. These rafts are constructed from two parallel canoes bridged by a wooden platform, which supports a pump equipped with a 3″–4″ suction hose. Sediments from the riverbed are extracted via the suction hose and processed on the raft. The processing involves a container that houses a sieve to separate coarse materials and a trough lined with mats to capture gold particles. Once separated by the sieve, the coarse materials are manually removed and stacked on the adjacent riverbank, colloquially termed the "beach." The finer particles that pass through the sieve are channeled back into the river by water flowing through the trough. While these fine particles are returned to the river, the gold is retained within the mats due to its high density, effectively separating it from other materials (Álvarez et al., 2011).

In highly mechanized mines, mining operators rely on large capital investments to purchase or rent heavy machinery. This machinery consists of front loaders, backhoes, and dump trucks. Most work fronts have a cutting height between 20 and 50 m. and the miners in the area mention that it would be necessary to deepen between 10 and 20 m. to reach the base rock or exploitable limit (Álvarez et al., 2011). Artisanal and small-scale miners often lack the financial capacity to secure mining equipment and supplies for extraction. As a result, they will often secure financing in advance from illicit sources, including unscrupulous gold traders and processors, "drop-by-drop lenders", and criminal organizations engaged in drug trafficking, extortion, and other illegal revenue-generating activities (OAS-DTOC (Organization of American States (OAS) - Department against Transnational Organized Crime (DTOC), 2021).

In both cases, the equipment uses diesel or gasoline fuel and emits significant amounts of CO_2. By considering the average utilization of the equipment, we can calculate the emissions for a day of operation. To do so, power emission factors were multiplied by the hourly consumption of the equipment (Michelin, 2023). Using the assumption of 16-hour workdays with a constant electricity supply (24 h), we calculated the CO_2 emission values of the equipment typically used in these operations. These calculations can be observed in Table 3.

In our analysis, similar to (Caballero Espejo et al., 2018), we differentiate between two types of mining operations based on their level of mechanization and location: minimally mechanized and highly mechanized. Minimally mechanized mining is further subdivided into operations occurring at riverbanks and those on riverbeds. At riverbanks, miners typically use smaller pumps and sieves to process the sediment for gold. Conversely, riverbed operations often involve using barges equipped with larger pumps, which allow deeper river extraction. These distinct setups imply different equipment types and quantities, as well as extraction capacity scales, influencing their respective CO_2 emissions. For our calculations, we separately estimated the emissions for riverbank and riverbed operations within the minimally mechanized category. Then we averaged these estimates due to the indistinguishable nature of these operations within our data source.

Highly mechanized mining, on the other hand, is characterized by the extensive removal of soil in plains or placer deposits—areas where gold has settled over many years. This process is markedly different from riverine operations and involves heavy machinery capable of moving large volumes of earth to access lower ore grades. Given the substantial equipment and energy requirements, the CO_2 emissions from highly mechanized mining are estimated based on the scale and intensity of these land-based operations.

There are no available sources that clarify the work schedules of these mines. Considering that the mines around this region contain gold in low grades, the operations should remain mostly constant. Thus, we assumed both types of operations work 26 days a month (312 days a year), considering holidays and interruptions, with a constant electricity supply (360 days).

For highly mechanized mining operations, we have estimated a daily fuel supply by tanker trucks to sustain the continuous and intensive energy demands. In contrast, the fuel supply is more sporadic for

Table 3
Typically used equipment in the region for ASGM activities and their power emissions factors.

Equipment	Fuel consumption	Work time	Emission factor	Total emissions† *
	Liters/Hour	Hours/ Day	Kg CO_2 / Liters	Kg CO_2/Day
25 HP gasoline pulp pump	5.7	16	2.32	211.49
90 HP Diesel pulp pump	7.98	16	2.69	343.46
110 HP Diesel pulp pump	9.2	16	2.69	395.97
23.50 ton Diesel truck	8.2	16	2.69	352.93
1.00 m3 Diesel backhoe	8.89	16	2.69	382.63
3.20 m3 Diesel front loader	12.52	16	2.69	538.86
18,000 liters Fuel tanker	8.2	16	2.69	352.93
Diesel electric generator	0.5	24	2.69	32.28

† *Total Emission = Fuel Consumption * Work Time * Emission Factor*.
* The decimal values may vary due to rounding.

minimally mechanized mines, which have lower energy requirements due to their smaller-scale pumping capacity and reliance on fuel-fed electric generators. We anticipate that these operations will require a monthly fuel supply of approximately six days. This supply chain typically involves a process known as 'swarming,' a method traffickers use to circumvent checkpoints and deliver fuel to illegal retail outlets serving the mining areas. Tanker trucks deliver fuel daily to these illicit points of sale, from which the fuel is distributed in smaller quantities, often in barrels of 13 gallons each, carried by hand to evade law enforcement detection (Mongabay, 2023). The Calculations can be observed in Table 4.

We calculate that in our study area, highly mechanized mines span an area of over 409.46 Km^2, and minimally mechanized mines span an area of over 510.18 Km^2. We estimated that the size of a single highly and minimally mechanized mine (*MA*) is 15 Km^2 and 5 Km^2, respectively, and we then divided the total area (*TA*) into these and multiplied by the yearly estimated amount of CO_2 emission (*YE*) of mine type:

$$Total\ Emission\ from\ Mining = YE * \frac{TA}{MA}$$

Consequently, we obtained the emission values of 20,503 Mg (t) CO_2/Year and 22,279.6 Mg (t) CO_2/Year for highly and minimally mechanized mines, respectively.

Table 4
Emission estimates of different mine types.

HIGHLY MECHANIZED MINE SITE (15 Km^2)				
Equipment	**Quantity**	**Workdays**	**Daily emissions**	**Yearly emissions**†
		Days/Year	Kg CO_2/Day	Mg (t) CO_2/Year
3.20 m3 Diesel front loader	1	312	538.86	168.1
1.00 m3 Diesel backhoe	1	312	382.63	119.4
23.50 ton Diesel truck	3	312	1058.78	330.3
18,000 liters Fuel tanker	1	312	352.93	110.1
Diesel electric generator	2	360	64.56	23.2
			Total	**751.1**
Minimally mechanized mine site - River bank (5 Km^2)				
Equipment	**Quantity**	**Workdays**	**Daily emissions**	**Yearly emissions**†
		Days/Year	KG CO_2/Day	Mg (t) CO_2/Year
25 HP gasoline pulp pump	2	312	423.17	132.0
90 HP diesel pulp pump	1	312	343.46	107.2
18,000 liters Fuel tanker	1	72	352.93	25.4
Diesel electric generator	1	360	32.28	11.6
			Total	**276.2**
Minimally mechanized mine site - River bed (5 Km^2)				
Equipment	**Quantity**	**Workdays**	**Daily emissions**	**Yearly emissions**†
		Days/Year	KG CO_2/Day	Mg (t) CO_2/Year
110 HP diesel pulp pump	1	312	395.97	123.5
18,000 liters Fuel tanker	1	72	352.93	25.4
Diesel electric generator	1	360	32.28	11.6
			Total	**160.5**

† *Yearly Emission* = *Quantity* ∗ *Work Days* ∗ *Daily Emissions*.

2.3.3.2. Transportation emissions. The Interoceanic highway in the Perúvian section comprises five sections from San Juan de Marcona to Iñapari. For the present study, we included the section between Inambari and Iñapari (on the border with Brazil), which covers a 403 km distance. The emission calculations were performed for two types of vehicles: light vehicles (personal vehicles) and heavy vehicles (buses, trucks, trailers, etc.). Given the variety of vehicles and brands that transit, an average of 8 L/100Km gasoline and 40 L/100Km of diesel consumption was assumed for light and heavy vehicles, based on the estimations of (International Energy Agency, 2019) and (Bureau of Transportation Statistics, 2023), respectively. Using the per liter emission factors mentioned above, yearly total emissions were calculated in Table 5, using the number of vehicles on the road between 2012 and 2021.

2.4. Calculation of net carbon emissions

Mining operations and transportation are significant contributors to CO_2 emissions within the region. However, the adverse impact of these emissions is compounded by deforestation, which not only adds to CO_2 levels through the decay of felled trees but also results in the loss of the forest's ability to sequester CO_2 from the atmosphere. This process is critical because trees act as carbon sinks, absorbing CO_2 as they grow. By quantifying both the emissions from mining and transportation and the decrease in CO_2 capture due to deforestation, we comprehensively assess the total net carbon emissions attributable to these activities. This assessment is crucial in understanding the full environmental impact of mining and deforestation, and it is vital for devising strategies to achieve net-zero carbon emissions. Net-zero carbon refers to balancing the amount of emitted CO_2 with an equivalent amount sequestered or offset, and it is a key target for mitigating the worst impacts of climate change.

3. Results and discussion

Our study found that the total carbon content within the area ranges from 15.8 to 46.2 Teragrams (Tg), with an average of 28.1 Tg. This equates to a carbon density of 9.12 to 26.67 megagrams (Mg) per hectare, averaging 16.22 Mg/ha. Deforestation has led to the removal of approximately 0.89 to 2.33 Tg of this carbon content—1.48 Tg in the average case—. Using the equation in Section 2.3.2, this amount of carbon content can be translated into a loss of 64.96 to 170.90 gigagrams (Gg) —**108.4 Gg** at the average case— of potential CO_2 capture each year.

Our estimates of CO_2 emissions from mining activities, given in Section 2.3.3.1, indicate that minimally mechanized operations contribute **22.3 Gg** annually, higher than the **20.5** Gg attributed to highly mechanized mining operations. This comparison underscores the relatively greater impact of minimally mechanized mining on CO_2 emissions.

Table 5
Vehicle traffic and emissions of Interoceanic highway, Inambari - Iñapari sections between 2012 and 2021.

Year	**Light vehicles**		**Heavy vehicles**	
	Number/Year	Mg(t) CO_2/Year	Number/Year	Mg(t) CO_2/Year
2012	100,000	7573	401,000	172,590
2013	147,000	11,133	546,000	234,998
2014	145,000	10,981	518,000	222,947
2015	149,000	11,284	563,000	242,315
2016	180,000	13,632	667,000	287,077
2017	190,000	14.389	669,000	287,938
2018	213,000	16,131	737,000	317,205
2019	206,000	15,601	692,000	297,837
2020	181,000	13,707	561,000	241,454
2021	253,000	19,160	811,000	349,054
Average	176,400	13,359	616,500	265,342

Furthermore, the transport sector also contributes significantly to the region's CO_2 emissions. Light vehicles are estimated to emit **13.4 Gg** of CO_2, while heavy vehicles contribute a substantial **265.3 Gg** as stated in Table 5. In total, transportation accounts for 278.7 Gg of CO_2 emissions annually.

Combining these figures, the total net CO_2 emissions from mining, deforestation (on average), and transportation activities in the study area are approximately 429.9 Gg (thousand metric tonnes) annually. A detailed breakdown of these emissions is provided in Table 6.

Our study's per hectare carbon content estimate of 16.22 Mg/ha contrasts with the higher figures of 91.9 Mg/ha and 83.9 Mg/ha reported by (Asner and Tupayachi, 2016) and (Csillik and Asner, 2020), respectively. Such discrepancies are understandable, given the divergent methodologies employed by each study. Our results still fall within the proposed ranges, affirming our approach's validity. Aggregating our carbon content figures with additional sources of emissions, we identify that the region is facing substantial environmental impacts, with total CO_2 emissions reaching 429.9 Gg annually. This significant level of emissions underscores the urgent environmental concerns in the area.

Mining is a significant source of emissions. However, as highlighted in Table 6, it only contributes 10 % of the total emissions. Nevertheless, the combined impacts of deforestation and regional development, directly influenced by the increase of mining operations, result in approximately six times higher emissions than mining operations itself. These emissions can only be counted indirectly towards mining.

The main drawback is the absence of a count on the total number of mines in the area. Instead, we have to estimate each mine by its area. The Geological, Mining, and Metallurgical Institute of Perú (INGEMMET) provides the mining concessions in the area. However, they do not match the observed mines as 65 % are out of concessions (Elmes et al., 2014) or several small concessions gather up to operate as one larger mine. Data on a clear distinction of these mines will provide better inputs for estimating mining emissions. Furthermore, tree observations are not distributed evenly in the study area, causing possibly larger deviations, and models for estimating the carbon content and capture loss are limited. Nonetheless, the results clearly imply that the development of the mining industry has severe environmental effects.

Mining is a temporary industry as the exploitable gold content is limited, causing the industry to move to another feasible source of gold when the current mine is exhausted. As it is a foreseeable future, closure planning of mining operations and reclamation of mine areas need to be carefully planned.

It is worthy to highlight the contamination of mercury in the region due to ASGM activities (Diringer et al., 2020) and the ASGM industry being the largest source of anthropogenic mercury emissions in the world (UN Environment, 2019); thus, the environmental aspects are not limited with carbon emissions.

The findings of our study underscore the environmental impact of artisanal and small-scale gold mining (ASGM) activities in the region, particularly in terms of carbon emissions. Although emissions directly from mining operations are significant, the data shows that approximately 90 % of emissions are attributable not to the mining itself but to associated activities such as transportation and the deforestation driven by the expansion of mining. In an era where combating climate change is critical, the unsustainable land use and production practices addressed by this study are untenable. It is essential to be aware of these indirect contributors to carbon emissions to mitigate the environmental degradation caused by ASGM activities.

Table 6
Sources and distribution of CO_2 emissions.

Source	Amount (Gg CO_2/Year)	Percentage
Deforestation	108.4	25.22 %
Minimally mechanized mining	22.3	5.19 %
Highly mechanized mining	20.5	4.77 %
Light vehicles	13.4	3.12 %
Heavy vehicles	265.3	61.71 %
Total	429.9	100 %

Based on our findings, on the path to net-zero emissions, we recommend that local and central governments and international organizations promote the establishment of less carbon emission-intensive modes of transport infrastructure to mining and industrial areas, establish a comprehensive plan for mine closure and reclamation in the areas, and the opportunity for reforestation with native species that have a higher potential for carbon capture. Additionally, as our results indicate, minimally mechanized mines cause higher emissions than highly mechanized ones. Bearing this in mind, process efficiency can be improved by increasing the mechanization of mining facilities, as (Fritz et al., 2023) also highlights.

However, we also underline that these environmental effects, especially mercury contamination, degradation of ecosystems, loss of biodiversity, and their concomitant risks to human well-being, are not irreversible and should be examined separately in further studies.

4. Conclusion

Our comprehensive study has quantified the significant environmental impact of artisanal and small-scale gold mining (ASGM) activities in the Madre de Dios region, with the resulting net CO_2 emissions being a substantial concern. Although direct emissions from mining operations contribute to these figures, the predominant sources of emissions are the collateral activities, mainly deforestation and transportation, driven by the expansion of mining. ASGM results in significant deforestation, converting forests into mining areas. This leads to biomass loss and reduces the area's ability to capture carbon. The study calculates a loss of 64.96 to 170.90 Gg of potential CO_2 capture annually due to deforestation from mining activities. Moreover, the construction and use of the Interoceanic Highway advanced access to mining areas, leading to increased CO_2 emissions from transportation. Light and heavy vehicles produce 278.7 Gg of CO_2 emissions each year, underscoring the importance of transportation in the region's overall emissions. This underscores the complex challenges faced in the quest to mitigate climate change impacts and the need for sustainable land use and production practices.

The paper suggests prompt and efficient reclamation actions to address environmental degradation, such as planting native trees with high carbon content. These endeavors are crucial for lessening the current effects and aligning with worldwide initiatives toward achieving net-zero emissions. Despite the substantial emissions from mining operations, this study indicates that most emissions stem from related activities like transportation and deforestation linked to mining growth. Taking a comprehensive approach to tackling the environmental impacts of ASGM operations is crucial, considering issues such as mercury pollution and the decline in biodiversity.

Implementing sustainable strategies is imperative to moving towards net-zero emissions. These should include promoting less carbon-intensive transportation, planning for mine closures and reclamation, and reforestation with carbon-dense native species. Our findings are a critical reminder of the indirect contributors to carbon emissions and the urgency of addressing these to curtail further environmental degradation. Moreover, the study highlights that addressing these issues holistically, including mercury contamination and biodiversity loss, is crucial for the well-being of ecosystems and human communities alike.

Funding

Funding for this research was provided by the National Science Foundation (Grant number 2039980). Any opinions, findings, and conclusions or recommendations expressed in this material are those of the authors and do not necessarily reflect the views of the National Science Foundation.

CRediT authorship contribution statement

Umut Mete Saka: Writing – original draft, Visualization, Software, Methodology, Investigation, Formal analysis, Data curation, Conceptualization. **Klaus Pacheco-Hague:** Methodology, Investigation, Formal analysis, Data curation. **Sebnem Duzgun:** Writing – review & editing, Validation, Supervision, Methodology, Funding acquisition, Conceptualization. **Nicole Smith:** Writing – review & editing, Validation, Funding acquisition.

Declaration of interests

The authors declare that they have no known competing financial interests or personal relationships that could have appeared to influence the work reported in this paper.

References

Álvarez, J., Sotero, V., Brack Egg, A., & Peralta, C.I. (2011). Mineria Aurífera en Madre de Dios y Contaminación Con Mercurio. http://siar.minam.gob.pe/puno/sites/default/files/archivos/public/docs/mineria_aurifera_en_madre_de_dios.pdf.

Aranoglu, F., Flamand, T., Duzgun, S., 2022. Analysis of artisanal and small-scale gold mining in peru under climate impacts using system dynamics modeling. Sustainability 14 (12), 7390. https://doi.org/10.3390/su14127390.

Asner, G.P., Powell, G.V.N., Mascaro, J., Knapp, D.E., Clark, J.K., Jacobson, J., Kennedy-Bowdoin, T., Balaji, A., Paez-Acosta, G., Victoria, E., Secada, L., Valqui, M., Hughes, R.F., 2010. High-resolution forest carbon stocks and emissions in the Amazon. Proc. Natl. Acad. Sci. U.S. A. 107 (38), 16738–16742. https://doi.org/10.1073/pnas.1004875107.

Asner, G.P., Tupayachi, R., 2016. Accelerated losses of protected forests from gold mining in the Peruvian Amazon. Environ. Res. Lett. 12 (9), 094004 https://doi.org/10.1088/1748-9326/aa7dab.

Avalos, G., Cambronero, M., Alvarez-Vergnani, C., 2022. Allometric models to estimate carbon content in Arecaceae based on seven species of neotropical palms. Front. in Forests and Global Change 5. https://doi.org/10.3389/ffgc.2022.867912.

Balslev, H., 2016. Aarhus University Palm Transect Database (7.1). Department of Bioscience, Aarhus University. GBIF.org.

Bureau of Transportation Statistics. (2023). Combination truck fuel consumption and travel. https://www.bts.gov/browse-statistical-products-and-data/freight-facts-and-figures/combination-truck-fuel-consumption.

Caballero Espejo, J., Messinger, M., Román-Dañobeytia, F., Ascorra, C., Fernandez, L., Silman, M., 2018. Deforestation and forest degradation due to gold mining in the peruvian amazon: a 34-year perspective. Remote Sens. (Basel) 10 (12), 1903. https://doi.org/10.3390/rs10121903.

Csillik, O., Asner, G.P., 2020. Aboveground carbon emissions from gold mining in the Peruvian Amazon. Environ. Res. Lett. 15 (1), 014006 https://doi.org/10.1088/1748-9326/ab639c.

Diringer, S.E., Berky, A.J., Marani, M., Ortiz, E.J., Karatum, O., Plata, D.L., Pan, W.K., Hsu-Kim, H., 2020. Deforestation due to artisanal and small-scale gold mining exacerbates soil and mercury mobilization in Madre de Dios, Peru. Environ. Sci. Technol. 54 (1), 286–296. https://doi.org/10.1021/acs.est.9b06620.

Elmes, A., Yarlequé Ipanaqué, J.G., Rogan, J., Cuba, N., Bebbington, A., 2014. Mapping licit and illicit mining activity in the Madre de Dios region of Peru. Remote Sens. Lett. 5 (10), 882–891. https://doi.org/10.1080/2150704X.2014.973080.

Environmental Protection Agency. (2023). Emission factors for greenhouse gas inventories.

Espin, J., Perz, S., 2021. Environmental crimes in extractive activities: explanations for low enforcement effectiveness in the case of illegal gold mining in Madre de Dios, Peru. The Extractive Industries and Society 8 (1), 331–339. https://doi.org/10.1016/j.exis.2020.12.009.

Fritz, B., Peregovich, B., da Silva Tenório, L., da Silva Alves, A.C., Schmidt, M., 2023. Mercury and CO2 emissions from artisanal gold mining in Brazilian Amazon rainforest. Nat. Sustain. 7 (1), 15–22. https://doi.org/10.1038/s41893-023-01242-1.

Henderson, Andrew, Galeano, Gloria, Bernal, Rodrigo, 1995. Field Guide to the Palms of the Americas. Princeton University Press.

International Energy Agency. (2019). Fuel economy in major car markets: technology and policy drivers 2005-2017. https://www.iea.org/reports/fuel-economy-in-major-car-markets.

Isaza, C., Bernal, R., Galeano, G., Martorell, C., 2017. Demography of Euterpe precatoria and Mauritia flexuosa in the Amazon: application of integral projection models for their harvest. Biotropica 49 (5), 653–664. https://doi.org/10.1111/btp.12424.

Leiva, J.D., 2022. Appropriate technologies and the geosocial evolution of informal, small-scale gold mining in Madre de Dios, Peru. The Extractive Industries and Society 12, 101165. https://doi.org/10.1016/j.exis.2022.101165.

Michelin. (2023). How to calculate your fleet's CO2 emissions. https://connectedfleet.michelin.com/blog/calculate-co2-emissions#:~:text=One%20litre%20of%20diesel%20creates,has%20emitted%20in%20a%20month.

Mongabay. (2023). Fuel trafficing sustains illegal mining in Peru's Madre de Dios. https://news.mongabay.com/2019/07/fuel-trafficking-sustains-illegal-mining-in-perus-madre-de-dios/.

Nicolau, A.P., Herndon, K., Flores-Anderson, A., Griffin, R., 2019. A spatial pattern analysis of forest loss in the Madre de Dios region, Peru. Environ. Res. Lett. 14 (12), 124045 https://doi.org/10.1088/1748-9326/ab57c3.

OAS-DTOC (Organization of American States (OAS) - Department against Transnational Organized Crime (DTOC). (2021, November). On the trail of illicit gold proceeds: strengthening the fight against illegal mining finances - Peru. https://www.oas.org/en/sms/dtoc/docs/On-the-trail-of-illicit-gold-proceeds-Peru-case.pdf.

Salo, M., Hiedanpää, J., Karlsson, T., Cárcamo Ávila, L., Kotilainen, J., Jounela, P., Rumrrill García, R., 2016. Local perspectives on the formalization of artisanal and small-scale mining in the Madre de Dios gold fields, Peru. The Extractive Industries and Society 3 (4), 1058–1066. https://doi.org/10.1016/j.exis.2016.10.001.

Swenson, J.J., Carter, C.E., Domec, J.-C., Delgado, C.I., 2011. Gold mining in the Peruvian Amazon: global prices, deforestation, and mercury imports. PLoS ONE 6 (4), e18875. https://doi.org/10.1371/journal.pone.0018875.

UN Environment. (2019). Global mercury assessment 2018. Global Mercury Assessment 2018 | UNEP. https://www.unep.org/resources/publication/global-mercury-assessment-2018.